[1]Tanvi U. Upadhyay
[2]Dr. J. G. Jamnani

Assessing Power Quality of Large-Scale Photovoltaic Sources Interconnected Distribution Systems Utilising Hybrid Energy Storage-based Custom Power Device

Journal of Electrical Systems

Abstract: -Non-conventional energy sources are becoming more prevalent because they discharge little to no carbon dioxide. As the world's population grows, technological advances and power requirements increase. Renewable energy sources (RES) are integrated into conventional systems to meet this demand. Despite its benefits, this interconnectivity affects the reliability and security of the power grid. The most significant concerns are power-quality issues, impacting consumer devices, and grid system operations. This study presents a simulated investigation of the effects of solar energy systems (PV) on the electric power quality of a distribution network using a Modified IEEE 33 Node Radial Distribution Test System. This article addresses power quality concerns such as voltage and power fluctuations, voltage profiles, and harmonics. Hybrid energy storage-based distributed STATCOM improves the voltage profile, voltage and power variations, and system harmonics. A battery supercapacitor is used as hybrid energy storage. The simulation analysis was performed using the MATLAB/Simulink environment.

Keywords: PV System, Large Scale Penetration, Power Quality Issues, Hybrid Energy Storage, Custom Power Device

I. INTRODUCTION

Renewable Energy Sources (RES), also known as Green Energy Resources, play a vital role in energy conversion because they generate energy from natural sources, such as solar insolation, wave currents, wind speed, geothermal energy, and water energy. RES produces little to no carbon footprint during power generation, which lowers the environmental impact by encouraging a safer environment [1]. The inherent reliability of renewable energy resources stems from their reliance on natural resource replenishment. Solar photovoltaics convert sunlight into electricity using photon energy, without endangering the atmosphere. Wind energy involves wind turbines and electrical generators, which produce electricity from kinetic energy generated from wind speed. Furthermore, the utilization of RES encourages economic and technological growth, making renewable energy resources an integral part of the worldwide sustainable energy development infrastructure [1]. As stated by the Central Electricity Authority of India, the total installed capacity was 441.96 GW in March 2024 [2]. Fossil fuel contributes around 210.96 GW and RES contributes 143.64 GW i.e. around 33% of 441.96 GW (Fig.(1)). Energy generation from other sources, such as gas, diesel, nuclear power, and hydropower, contributes 19% of 441.96 GW as shown in Fig. (1).

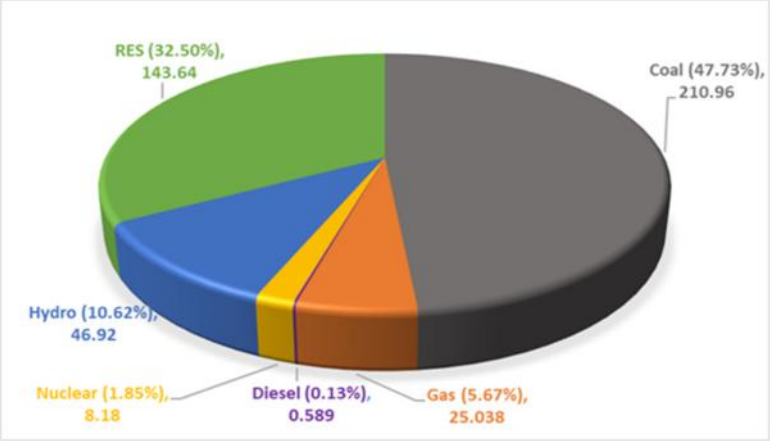

Fig.1 Installed Capacity of Energy Sources in India on March 2024 [2]

Introducing clean energy sources into the grid creates worries about power quality, such as harmonic distortions and voltage-related issues. System interruptions and the unpredictable nature of renewable source (RES) generation cause power characteristics such as sagging, swelling, and voltage changes. Power electronic converters, key component of renewable energy systems, generate harmonics [3]. These concerns are divided into grid-side and renewable energy categories. The unpredictable and uncontrollable behavior

[1] *Corresponding author: Research Scholar, Dept. of Electrical Engineering, Pandit Deendayal Energy University, Gandhinagar, India
[2] Associate Professor, Dept. of Electrical Engineering, Pandit Deendayal Energy University, Gandhinagar, India

of wind and photovoltaic (PV) solar systems causes RES systems to produce inconsistent outcomes. Unpredictability impacts system voltage, resulting in fluctuations, swells, and sags.

These challenges can be divided into two categories: grid-related concerns and RES-specific concerns. The intermittent nature of RES generation on the grid disrupts the supply-demand balance, resulting in voltage imbalances, frequency aberrations, and decreased system reliability. According to the RES-specific perspective, the variability in power output becomes severe because of the stochastic nature of wind and photovoltaic (PV) systems. RES depends upon naturally fluctuating environmental elements like wind speed and solar radiation, in contrast to conventional production, which has an output that is comparatively steady and predictable. Grid management is made more difficult by this variability, which causes frequent and notable variations in voltage levels. Short-term drops in voltage magnitude are known as voltage sags, and they frequently happen when load demand is strong or when RES output is abruptly reduced. On the other hand, sudden load disconnections or RES overgeneration during low demand can cause voltage swells, which are characterized as brief rises in voltage. Furthermore, power electronic converter causes harmonics, and has the potential to spread across the grid, interacting with other electrical devices and exacerbating problems with power quality. The sinusoidal waveform of the grid voltage and current is distorted by these harmonics, which can result in higher losses, equipment overheating, and possible faults in systems.

Table 1 Literature Review on Power Quality Improvement Techniques

Paper	Technique Used	RES Used	Key Contributions
[7]	Custom Power Device – D-STATCOM	Photovoltaic System	Proposed combined parallel VSI and DC link-fed D-STATCOM configuration Improves power regulation and reduces voltage fluctuations
[8]	Custom Power Device – DVR	Photovoltaic System	Reactive Power Compensation and Voltage Regulation Active Power Tracking is also employed in an article
[9]	Energy Storage – Battery	Photovoltaic System	Improves voltage regulation and reduces power fluctuations Optimizes power consumption using a meta-heuristic approach
[10]	Energy Storage – Supercapacitor	Photovoltaic System	Smoothing of Power Improvement in the Stability of Power System
[11]	Energy Storage – Supercapacitor	Photovoltaic System	Improvement in power quality parameters like voltage and power Comparison of PID controller-based control system and fuzzy logic-based control system in terms of power quality
[12]	Battery with D-STATCOM	Photovoltaic System	Improves voltage-related power quality issues Proposed three-stage control framework for battery-based D-STATCOM
[13]	Battery – SC Hybrid ESS	Photovoltaic System	Mitigates voltage and frequency fluctuations Provides an algorithmic solution for sitting and sizing of HESS
[14]	Battery – SC Hybrid ESS	Photovoltaic System	Mitigates power and voltage fluctuations Uses bi-lateral DC-DC converter for control of HESS
[15]	Battery – SC Hybrid ESS	Photovoltaic System	Reduces power fluctuations → Employs novel power smoothing approach using HESS

Several studies have thoroughly examined the impacts of integrating RES into electrical distribution systems and their consequences for power quality [4-6]. The authors of [4] thoroughly analyze power quality issues that affect both AC and DC power systems. They also provided standards and mitigation strategies in their study. This study highlights the importance of power quality requirements to guarantee system

dependability. In [5], the focus is on the impacts of RES on microgrids, particularly concerning supra-harmonics in the system. The study also examines the effect of supra-harmonics and compares different types of methods for improving the power quality of the network. The [6] discusses the issues of incorporating RES into power systems. The authors analyze power quality issues and discuss several mitigating strategies. Their findings show the critical role of power electronic devices and FACTS (flexible AC transmission systems) devices, such as STATCOMs and UPFCs, in addressing these concerns. These devices are well known for their ability to improve system stability and power quality. An examination of the literature reveals a variety of strategies for improving the power quality of conventional power networks integrated with renewable energy sources, as shown in Table 1. Custom power devices, such as Distribution Static Compensators (D-STATCOM), Dynamic Voltage Restorers (DVR), and Unified Power Quality Conditioners (UPQC), are widely used to address voltage-related issues such as sags, swells, interruptions, fluctuations, and harmonics. These devices also help with reactive power compensation [7-8]. However, their shortcomings include their inability to effectively provide active power control or store surplus energy, as well as their failure to address frequency fluctuations [8]. Hybrid energy storage systems (HESS), which integrate two or more energy storage systems to enhance power quality characteristics, are a new strategy in the literature. According to studies, HESS—in particular, battery-supercapacitor (battery-SC) combinations—has proven effective in reducing some power quality problems, including power imbalances, harmonics, and voltage variations [9–12]. These studies, however, frequently deal with these problems separately rather than concurrently, which leaves gaps in attaining a thorough increase in power quality [13–15]. Hence, these power quality parameters are analysed and improved in this manuscript.

This article discusses the following topics. (1) A succinct description of how conventional power systems' power quality is impacted by large-scale RES integration. (2) This study examines the effects of PV systems on power quality issues, including voltage fluctuations, power and voltage fluctuations, and system harmonics. (3) The literature assessment concludes that while power quality can be enhanced to a certain extent with D-STATCOM or other customized power devices, it cannot be reduced to the IEEE/IS standards-recommended level. Furthermore, excess energy from RES sources cannot be stored by specialized power devices. Therefore, this work introduces the D-STATCOM, which is based on hybrid energy storage. (4) A custom power device based on a hybrid energy storage technology improved the system's power quality attributes. Also included are insights into the design and control strategies for HESS. (4) A conventional algorithm was used to regulate power between the PV, load, grid, and HESS. (5) By using H-STATCOM, power quality characteristics are improved, such as voltage and power fluctuations and harmonics being reduced, and voltage profile controls under dynamic situations are improved.

The remainder of this paper is organized as follows. Section 2 describes the traditional distribution system used in this study, the modeling of solar photovoltaics (PV), the comprehension and development of a hybrid energy storage-based STATCOM, and the power management of the PV, Grid, and Hybrid Energy Storage Systems. Section 3 discusses the findings and debates. The last section presents the conclusions of the study.

II. METHODOLOGY

A. Modified IEEE 33 Node Radial Distribution Test System

A revised IEEE 33-node radial distribution strategy is shown in Fig. (2). It consists of a single voltage source that serves as a substation and has a rating of 100 MVA and 66 kV. There is also a substation with an 8 MVA transformer value of 66 kV/11 kV. The 66 kV substation is indicated by Node 1. Nodes 2 through 18 were the 11 kV feeders. The distribution lines link them together. Nodes 4, 6, 8, 10, 12, and 14 are some of the six branches. Each branch had a power distribution transformer with a rating of 1600 kVA and 11 kV/0.433 kV. Nodes 19–27 were also 0.433 kV feeders. Nodes 28–33 were the load nodes. Both nonlinear and linear loads were taken into account. Table 2 presents the load parameters. A summary of the systems under question is shown in Table 3.

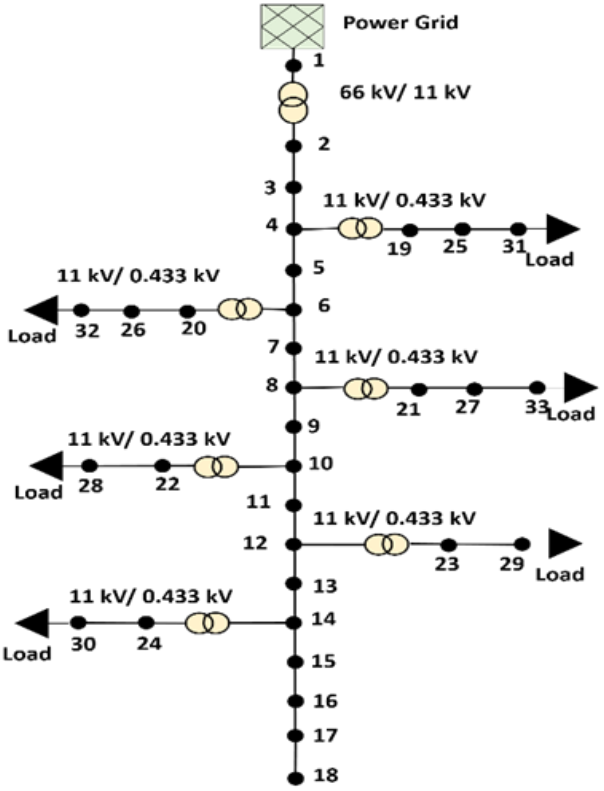

Fig. 2 One line Diagram of the System Under Study

Table 2 Load Parameters

Node	Phase A		Phase B		Phase C	
	P (kW)	Q (kVAR)	P (kW)	Q (kVAR)	P (kW)	Q (kVAR)
28	498.1	368.4	510.1	358.3	501.2	362.9
29	403.3	315.6	385.3	323.2	395.9	303.9
30	510.4	365.6	495.6	345.3	503.7	351.6
31	520.2	350.2	535.1	342.6	530.6	356.6
32	505.6	320.2	490.2	296.3	497.2	308.2
33	255.3	128.3	240.2	141.4	249.4	134.6
33	Rectifier - Non Linear Load – 332.6 kW, 297.5 kVAR					

Table 3 Summary of the System

Total Generators	3.217 MW	2.111 MVAR
Total Load	3.004 MW	2.103 MVAR
Total Losses	0.213 MW	0.008 MVAR
No. of Buses	33	-
No. of Branches	32	-
No. of Loads	7	-
No. of Substation	1	-

B. Modelling and Simulation of PV Array System

The solar photovoltaic energy system comprises a solar PV array and an inverter for grid connections. The mathematical modeling of the PV module is done using MATLAB/Simulink software. Eq. (1) produces the result I_{op} [7].

$$I_{op} = N_{cp}\left[I_{sc} + k_i(T-298)\frac{G}{100}\right] - N_{cp}I_0\left[exp^{\frac{N_{cp}V + I_{op}N_{cs}R_{se}}{N_{cp}N_{cs}V_t}} - 1\right] - \left[\frac{N_{cp}V + I_{op}N_{cs}R_{se}}{N_{cp}R_{pa}}\right] \quad (1)$$

$$I_0 = I_{rs}\left[\frac{T}{298}\right]^3 exp^{\frac{qV_t}{Ak\left(\frac{1}{T}-\frac{1}{298}\right)}} \quad (2)$$

$$V_t = \frac{kT}{q} \tag{3}$$

In Eq. (1), I_{sc} is the current passing through the photovoltaic module at short circuit condition (A), k_i is the temperature-dependent component for short circuit current, T is the ambient temperature, and the reference temperature is 298 K. Solar irradiance G is in W/m^2. The diode saturation current I_0 may be calculated using Eq. (2). The thermal voltage V_t may be calculated using Eq. (3) [7]. R_{se} is the PV module's equivalent series resistance. R_{se} must be below 0.01 times the open circuit voltage (V_{oc})/short circuit current (I_{sc}). The R_{pa} represents the PV module's equivalent shunt resistance. The shunt resistance should be higher than a thousand times the ratio of V_{oc} to I_{sc}. V is the PV module's output voltage. N_{cp} is the number of cells linked in parallel, whereas N_{cs} is the number of modules linked in series. A represents the coefficient of ideality of a PV cell. I_{rs} interprets the diode's reverse saturation current. Electron q has a charge of 1.602 × 10^{-19} C. Boltzmann's constant, k, is 1.38×10^{-23} J/K [8].

$$I_{op} = N_{pp}\left[I_{sc} + k_i(T-298)\frac{G}{100}\right] - N_{pp}I_0\left[exp^{\frac{N_{pp}V + I_{op}N_{ps}R_{se}}{N_{pp}N_{ps}V_t}} - 1\right] - \left[\frac{N_{pp}V + I_{op}N_{ps}R_{se}}{N_{pp}R_{pa}}\right. \tag{4}$$

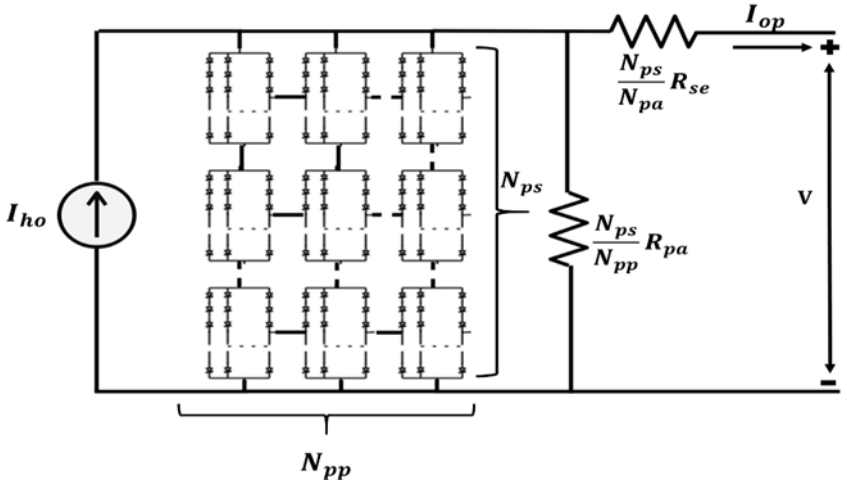

Fig. 3 Equivalent Model of Photovoltaic Array

Eq. (4) calculates the output current of the PV array: PV which is constructed by connecting the PV modules in series and parallel. Fig. (3) depicts the corresponding architecture of a photovoltaic (PV) array. N_{pp} is the number of PV modules linked in parallel and N_{ps} is the number of PV modules connected in series. A three-phase IGBT-based converter links the PV array system to the grid. The maximum power point tracking (MPPT) technique was implemented to obtain the maximum power from the PV array. The hill-climbing approach is used for MPPT [8].

Sinusoidal pulse-width modulation (SPWM) creates gate signals for IGBT switches. The inverter is controlled using a mechanism based on the D-Q coupling theory. Fig. (4) depicts a block schematic of the control approach. The model was simulated using Standard Test Conditions (STC, 25 °C, 1000 W/m^2).

The 240 W PV module from Waree Energies is considered to form a PV array. The total load of the considered system was 3.00 MW. Hence, the rating of the PV array must be 3.2 MW. The maximum power of the PV module was 240 W, open-circuit voltage was 37.8 V, and short-circuit current was 8.33 A. The voltage at maximum power is 29.65 V, and the current at maximum power is 7.82 A [9]. The DC link voltage of the PV array was set at 2.7 kV because the rated voltage of the distribution system was 11 kV. Using such a high voltage would require larger DC-link capacitors, inverters, and more solar panels in series to generate the same amount of power. This results in higher installation costs. Therefore, a lower DC link voltage was chosen and integrated with the distribution system using a step-up transformer. The total number of required PV modules and the number of panels required in series and parallel were determined using Eq. (5), Eq.(6) and Eq.(7) [9].

$$\text{Total required panels } N_T = \frac{\text{Total required capacity of PV Array}}{\text{Maximum Power of PV Module}} = \frac{3.2\text{ MW}}{240\text{ W}} = 13333 \tag{5}$$

$$\text{Total required panels in series } N_{ps} = \frac{\text{DC Link voltage of PV Array}}{\text{Voltage at Maximum Power}} = \frac{2500}{30.65} = 82 \tag{6}$$

$$\text{Total required panels in parallel } N_{pp} = \frac{\text{Total required Panels}}{\text{Panels required in Series}} = \frac{13333}{82} = 163 \tag{7}$$

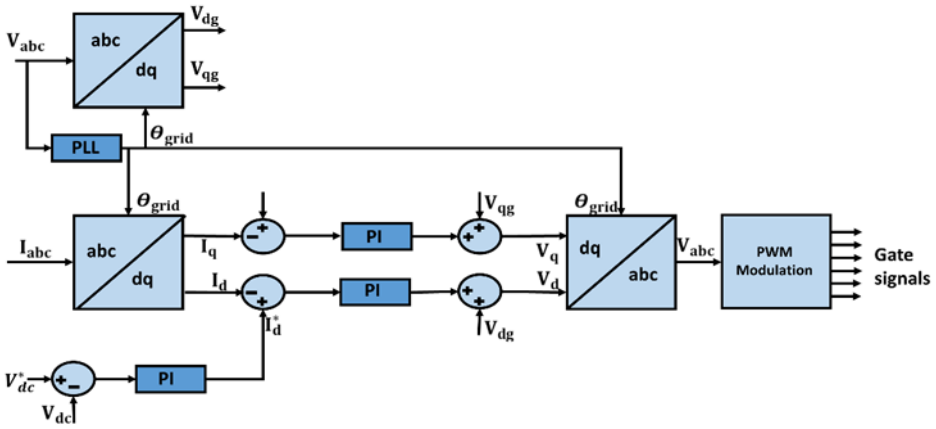

Fig. 4 Control of PV's Inverter [8]

Hence, a total of 13333 PV modules are required to produce 3.02 MW power from 240 W single solar modules. The 82 PV modules are arranged in a series to create a single string, and then 163 strings are connected in parallel to produce 3.2 MW.

The voltage at maximum power for the PV array (V_{M_PV}), the current at maximum power for the PV array (I_{M_PV}), the open circuit voltage (V_{OC_PV}) and the short circuit current of the PV array (I_{SC_PV}) are given as below [9].

V_{M_PV} = No. of panels in series * voltage at maximum power of single PV module = 82 * 29.65 = 2413.3 V

I_{M_PV} = No. of panels in parallel * current at maximum power of single PV module = 163*7.82 = 1274.6 A

V_{OC_PV} = No. of panels in series * open circuit voltage of single PV module = 82 * 37.08 = 3046.56 V

I_{SC_PV} = No. of panels in parallel * short circuit current of single PV module = 163 * 8.33 = 1357.79 A

Next, an inverter for the PV array system was designed. For the parameter design, the inverter efficiency is considered to be 90%. Hence, the required rating of the inverter output is, and the output power rating of the PV array/inverter efficiency is, 3.2 MW/0.9 = 3.5 MW. The maximum DC input voltage of the inverter is equal to the open-circuit voltage of the PV array [9]. The maximum DC input current of the inverter is the same as the sum of the short-circuit currents of all the parallel strings of the PV module. The maximum DC power of the inverter is the product of its maximum DC input voltage and maximum DC input current. The maximum AC output power of the inverter must be equal to or greater than the maximum DC power of the inverter [9]. The parameters for the PV array and PV inverter are listed in Table (4) and Table (5) respectively

Table 4 Parameters for PV Array

Parameters	Values		
Irradiance Level (W/m^2)	1000	600	200
MaximumPower (MW)	3.2	2.8	1.9
Optimum Operating Voltage (V)	2413.3	2382.1	2343.1
Optimum Operating Current (A)	1274.6	648.82	340.9
No. of modules in Series	82		
No. of modules in Parallel	163		

Table 5 Parameters for PV Inverter

Inverter Power Rating (MW)	3.5	Max. Output Current (A)	1748
Max. DC Input Voltage (V)	3040.56	Rated AC Power (MVA)	4.37
Max. DC Input Current (A)	1357.79	Nominal AC Voltage (kV)	2.5
Max. DC Power (MW)	4.1	AC Power Frequency (Hz)	50

C. Hybrid Energy Storage System (HESS) based Custom Power Device

HESS technology was created by combining two energy storage technologies with diametrically opposed features. Typically, it consists of one high-power-density energy storage unit and one high-energy-density system. Energy density was defined as the total energy density per unit volume. The rate at which energy is transferred per unit volume is referred to as power density. Batteries and fuel cells have low power densities but high energy [13].

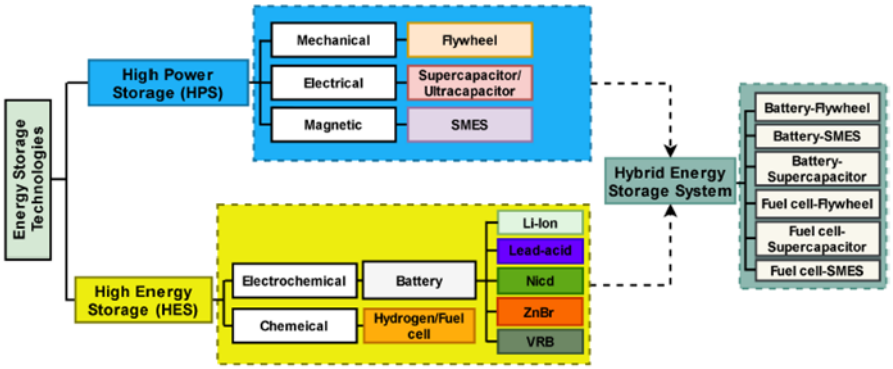

Fig. 6 HESS Various Combinations [13]

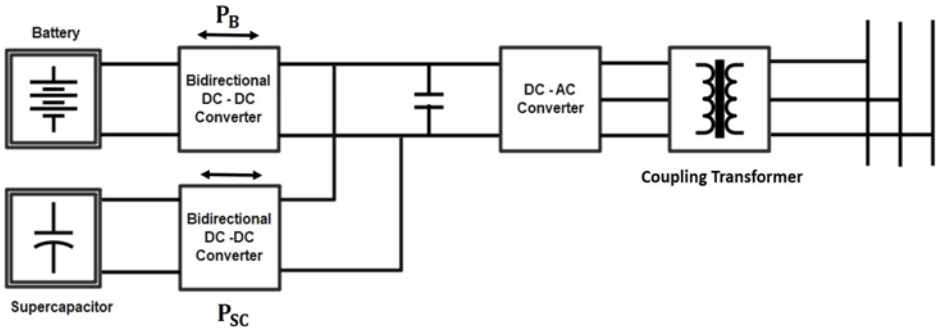

Fig. 7 Configuration of H-STATCOM

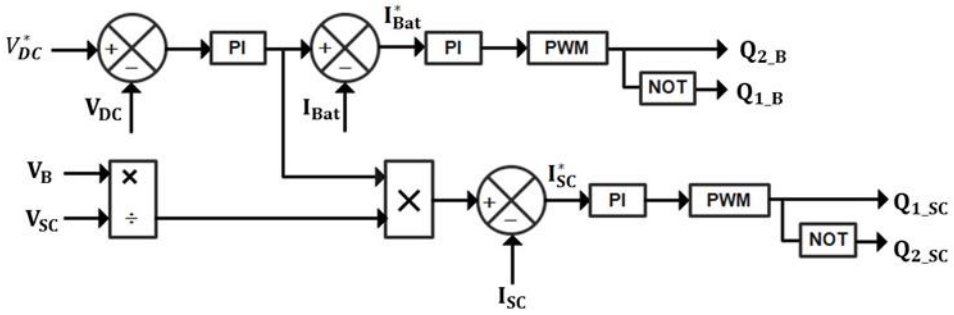

Fig. 8 Control Technique of Battery's and SC's DC-DC Converter [13]

Supercapacitors (SC) and flywheels offer high power density but low energy density. Thus, the following are used worldwide: batteries and fuel cells, batteries and flywheels, fuel cells and SC, and fuel cells and flywheels. The different HESS combinations are shown in Fig. (6) [13]. The battery-SC HESS is used in this study to lessen harmonics and changes in voltage, power, and frequency. The SC manages abrupt fluctuations in load and power transients, while the battery provide sustained power. This research refers to Battery-SC HESS-based D-STATCOM as H-STATCOM instead of regular D-STATCOM because of the following advantages [14].

(1) H-STATCOM provides a greater energy storage capacity than conventional capacitors or batteries. H-STATCOM allows the HESS to store more energy than either capacitors or batteries alone, even though it has a battery and SC. The additional energy that PV can generate during off-peak hours may therefore be stored by HESS and returned during times of high demand.

(2) H-STATCOM can provide energy storage, power quality improvement, and active-reactive power management of the system. Reactive power correction and real-time power quality improvements are provided by D-STATCOM. Additionally, the H-STATCOM controls voltage and frequency. The system became more reliable and adaptable as a result.

(3) The provision of a black-start facility is primarily dependent on the H-STATCOM. It temporarily offers stored power to restart the grid in the case of a malfunction or blackout. This problem is not improved by D-STATCOM.

Table 6 compares energy storage devices based on their energy density, power density, and storage efficiency. It is observed that the lithium-ion battery has the highest energy density, while the supercapacitor has the best power density of all energy storage devices. Furthermore, lithium-ion and SC have an efficiency

of approximately 80-97%. As a result, a lithium-ion battery and SC combination were used in this work. The H-STATCOM, which consists of a battery and SC in parallel, is depicted in Fig. (7).

Table 6 Various Energy Storage Comparison

Energy Storage	Efficiency (%)	Energy Density (Wh/L)	Power Density (W/L)
Flywheel	70 – 90	20 - 80	1000 – 5000
Supercapacitor	80 – 95	10 - 30	20000+
SMES (Superconducting Magnetic Energy Storage)	65 – 80	0.2 - 0.6	1000 – 4000
Lead – Acid Battery	75 – 90	50 – 120	10 – 400
Lithium – Ion Battery	90 – 95	200 – 500	1500 – 10000
Zinc – Bromine Battery	90 – 97	55 – 65	10 – 25
Vanadium – Redox Battery	90 – 98	15 – 25	5 – 15

Fig. (8) shows the battery and SC controls. H-STATCOM is controlled by SRF a Synchronous Reference Frame (SRF)-based control technique [14]. As shown in Fig. (8), when comparing the V_{DC} voltage with the reference DC link voltage V_{DC}^{*}, the error signal is fed to the PI controller, and the output from the PI controller is compared with the current of the battery. The signal from this comparison provided the reference current of the battery. The battery current and reference current are compared, and the error signal from that comparison is fed to the PWM block to generate the DC–DC-DC converter gate signals of the battery [14]. To control the SC DC-DC converter, the battery voltage to SC voltage ratio is multiplied by a battery reference current, which gives the reference current for the SC. The current from the SC and the reference current for the SC are compared, and an error signal is fed to the PI controller. The output of the PI controller is sent to the PWM block to generate the gate signal for the DC-DC converter associated with the SC [14]. The parameters of the H-STATCOM are listed in Table (7).

1. Sizing of Energy Storage System

Assumptions :

- For simplicity, the Hybrid STATCOM's DC link voltage is 2700 V, which is also the PV array's DC link voltage.
- The battery array and SC array have a combined power rating of 3.2 MW. The efficiency and derating factors of the battery cells are assumed to be optimal when they are in balanced conditions.
- The SC array's discharge rate is considered as one hour.
- The battery array's discharge rate is set as four hours.

a) Sizing of Supercapacitor (SC) Array)

SC cells typically operate between 2.5 V and 2.7 V. SC cells are typically coupled in series and parallel to provide high power delivery. A single SC cell has a rating of 2.7 V and a temperature range of 3000 F. The total energy to be supplied by the SC array is E_{SCt}, which is calculated using Eq. (8) [15].

$$E_{SCt} = \text{Discharge Rate} * \text{SC array total required power rating} = 11.52 \text{ NJ} \quad (8)$$

No. of SC cells required in the series is N_{SCS} is given by Eq. (9) [15].

$$N_{SCS} = \text{Voltage of SC array} = 1000 \quad (9)$$

For parallel configuration, calculate the total required capacitance of the SC array (C_{SCt}) by Eq. (10) and the no. of the SC cells required in parallel (N_{SCP}) is given by Eq. (11) [15].

$$C_{SCt} = \frac{E_{SCt}}{V_t^2} = 1580 \text{ F} \quad (10)$$

$$N_{SCP} = \text{array capacitance} \cong 0.52 \quad (11)$$

The number of SC cells cannot be fractional; hence, at least one SC cell is required in a parallel design.

b) Sizing of Battery Array

The voltage of the battery's single cell is 3.7 V with an energy capacity of 1 kWh. The required no. of battery cells in series is (N_{Bs}) is found using Eq. (12) [15].

$$N_{Bs} = \text{Voltage of Battery array} \cong 729.72 \quad (12)$$

The number of cells in a series can not be fractional; hence, the required number of battery cells in a series would be 730.

The total energy capacity required for the battery array would be given by E_{Bt} and given by Eq. (13) [15].

$$E_{Bt} = \text{Discharge Rate} * \text{Battery array power rating} = 12.8 \text{ MWh} \quad (13)$$

The no. of the battery cells required in parallel connection is N_{BP} and found using Eq. (14) [15].

$$N_{BP} = \frac{\text{Total energy required for the battery array}}{\text{The energy capacity of the battery array}} = 12800 \quad (14)$$

Therefore, the 3.2 MW battery array with a 2700 V rating required 730 battery cells in series and 12800 battery cells in parallel.

Table 7 Parameters of H-STATCOM

Parameters	Value
LV rating of the coupling transformer	2700 V
HV rating of the coupling transformer	11 kV
MVA rating of the coupling transformer	2000 kVA
Voltage of single module of Battery	3.7 V
Voltage of Battery Array	2700 V
Voltage of single module of SC	2.7 V
Voltage of SC Array	2700 V
DC link capacitance of H-STATCOM	396 µF
DC link voltage of H-STATCOM	2700 V
Ah rating of Battery	2000 mAh
Capacitance of Single module of SC	3000F
Capacitance of SC Array	1580 F

D. Power Management between PV, Grid, and Energy Storage

This article discusses a power management strategy that primarily distributes power flow between the load, grid, PV, SC, and battery. Power balancing is critical for managing the hybrid power system. It immediately ensures the stability of the hybrid power system. The power management algorithm, as seen in Fig. 9, is used for this purpose. It has six modes of operation. The modes are outlined below. SOC (state of charge) refers to the amount of charge accessible in energy storage at any particular time. The minimum State of Charge (SOC) limit is the point at which an energy storage device cannot release energy without causing damage or decreasing its life. This limit protects the battery or storage system from overdischarge, maintaining its longevity and correct operation. When the SOC reaches this limit, the system stops discharging and will only allow charging to bring the SOC above the minimum level. The maximum State of Charge (SOC) limit is the highest point at which an energy storage system (ESS) cannot be charged without risking overcharging, which can harm the battery's health and shorten its life. This limit guarantees that the storage system runs within safe parameters, preventing overcharging, which could result in overheating or other damage.

Operation of Mode 1 : As illustrated in Fig. (10), when the load demand exceeds the available solar power, verifying that the battery's state of charge (SOC) remains above its minimum threshold is necessary. If this condition is satisfied, the battery compensates for the power shortfall, as specified in Table (8). In this operational mode, the battery undergoes discharge, resulting in a gradual reduction in its SOC. The decrease from 94% to 93.83% indicates that the battery retains sufficient capacity to supply power for an extended

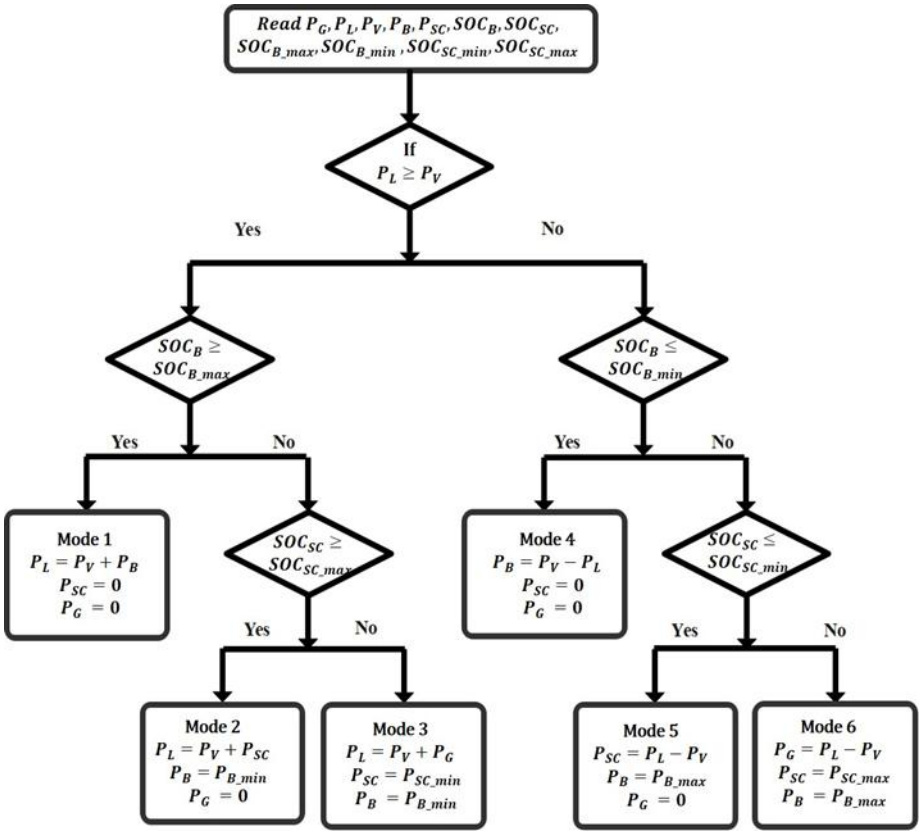

Fig. 9 Power Management Algorithm

duration. The supercapacitor (SC), being inactive during this phase, does not contribute to the power balance, with its power output remaining at zero and its SOC unchanged. The H-STATCOM maintains a constant DC link voltage of 330 V, while the grid neither supplies nor absorbs power, resulting in zero grid power contribution.

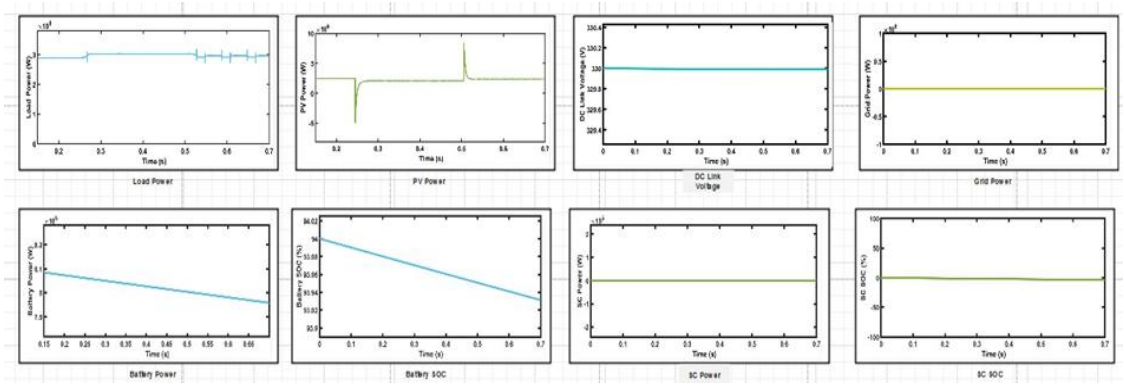

Fig. 10 H-STATCOM Operation – Mode 1

Table 8 H-STATCOM Operation

Mode	P_G (MW)	P_L (MW	P_V (MW)	$\Delta P = P_L - P_V$ (MW)	V_{DC} (V)	P_B (MW)	SOC_B	P_{SC} (MW)	SOC_{SC}
1	0	3.0	2.2	0.8	330	0.8	Decreasing	0	Constant
2	0	3.0	2.2	0.8	330	0	Zero	0.8	Decreasing
3	0.8	3.0	2.2	0.8	0	0	Zero	0	Zero
4	0	3.0	4	1	330	1	Increasing	0	Zero
5	0	3.0	4	1	330	0	Constant	1	Increasing
6	1	3.0	4	1	0	0	Constant	0	Constant

Operation of Mode 2 : The performance of the H-STATCOM in Mode 2 is shown in Fig. 12. When the load demand exceeds the PV power generation and the battery cannot provide the required energy, the system's controller switches to using the supercapacitor (SC). When the battery is found to be incapable of providing power, the SC takes over to supply the remaining power to the load, as long as its state of charge (SOC) exceeds the set minimum limit. Under these conditions, the SC will discharge to make up for the power deficit. In this state, the battery's SOC remains constant at 0% because it is not contributing to the energy supply. The SC, due to its intrinsic increased power density, can produce higher bursts of power over shorter periods of time, making it suited for correcting transitory power imbalances. This is shown in the dramatic decline in the SC's SOC, which falls from 95% to 59%. This dramatic decrease in SOC illustrates the SC's active role in discharging and supplying energy to the load during this phase of operation. The SC's ability to offer rapid power responses, albeit for shorter periods of time, is important to H-STATCOM operation in Mode 2, providing power supply stability when other energy sources fail to fulfill demand.

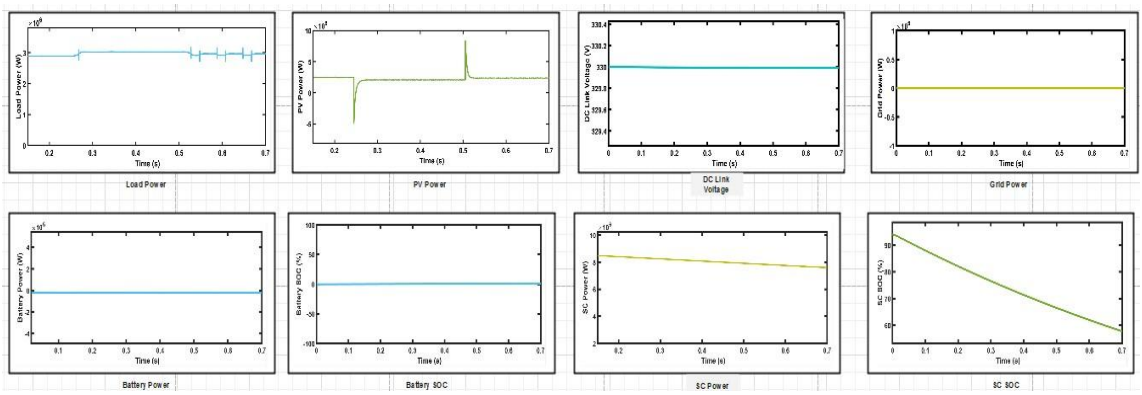

Fig. 11 H-STTCOM Operation – Mode 2

Operation of Mode 3 : Fig. (12), which shows the H-STATCOM performance in Mode 3, shows how the system behaves when the load demand is greater than the total power production of the PV, battery, and supercapacitor (SC). In this specific mode, the system encounters a situation in which none of these energy sources can provide the 0.8 MW of electricity needed to meet the load. Therefore, the remaining energy is sourced from the grid to make up for the power shortage. Due to inadequate charging levels, neither the battery nor the SC can provide any power in this mode, so their power outputs are essentially zero. Because of energy storage's states of charge (SOC) have dropped below their operational limits, the battery and the SC are not able to provide required load. As a result, the system switches to depending on the grid to supply the power required to balance the load. In this mode, the grid behaves as a backup energy source, making sure that, in the event that energy storage and renewable generation are insufficient, the overall demand for power is satisfied. This mode emphasizes how important grid integration is to H-STATCOM, as the grid acts as a dependable fallback to preserve system stability and a steady supply of energy, especially during times of high demand or when storage and renewable resources run out. This operational strategy improves the overall reliability and flexibility of the H-STATCOM by guaranteeing that the power system is stable even in situations where local renewable resources and energy storage technologies are unable to meet the load needs.

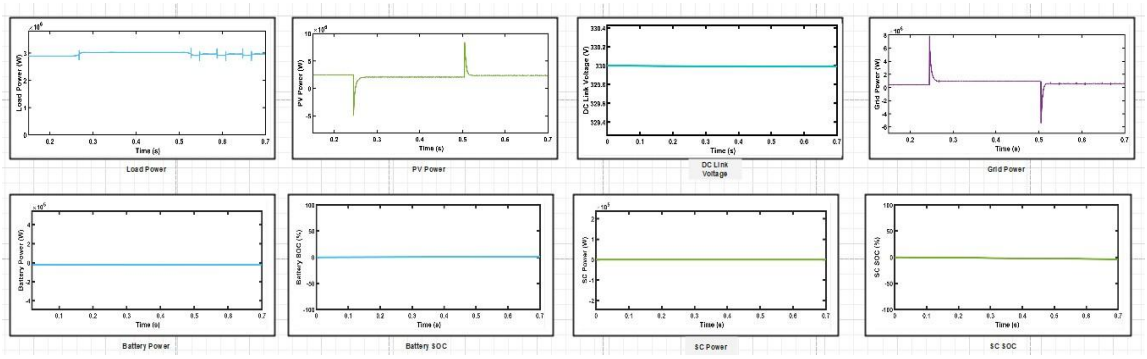

Fig. 12 H-STATCOM Operation – Mode 3

Operation of Mode 4 : The system has more available energy when the load power demand is less than the solar power generation, as shown in Fig. (13). According to Table (8), there is 1 MW of excess energy available in this case. The mismatch between generation and consumption—where the production of renewable energy surpasses the immediate load requirements—is the cause of this excess energy. As long as the battery's state of charge (SOC) stays below the highest advised limit, the system uses the extra energy to manage this excess and charge the battery. The system uses the excess energy to recharge the battery because its state of charge (SOC) is initially low. This causes the SOC to gradually rise from 0% to 12% during this operating phase. By ensuring that the available renewable energy is not lost and is instead conserved for later use, this charging procedure improves the system's overall efficiency. By giving battery charging top priority, the system maximizes energy use and helps preserve energy supplies for times when demand might outstrip supply. Since their involvement is not necessary, the grid and the supercapacitor (SC) are both inactive during this mode. The grid neither supplies nor absorbs energy, and the SC does not help with power balancing. As a result, the grid's and the SC's power outputs stay at zero. The H-STATCOM ensures continuous voltage management and operational stability by maintaining a steady DC connection voltage of 330 V throughout this procedure. The smooth transmission of energy between various components and the preservation of the system's integrity depend on this steady voltage.

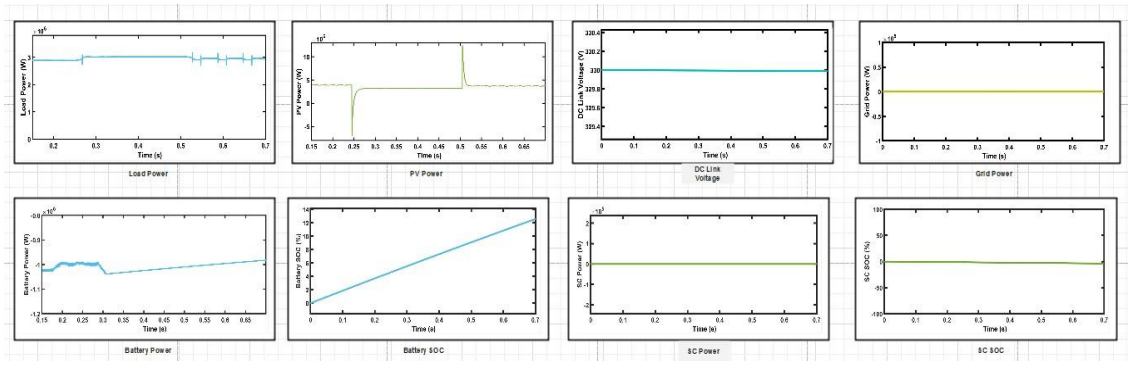

Fig. 13 H-STATCOM Operation – Mode 4

Operation of Mode 5 : There is an excess of accessible energy in the system when the load power is less than the PV power, as shown in Fig. (14). According to Table (8), there is 1 MW of excess electricity available in this scenario. Usually, the battery would be charged first using this extra energy. The battery cannot absorb any more energy if its state of charge (SOC) rises above the upper limit permitted. In these situations, the system must ensure the supercapacitor (SC) is ready to take in the extra energy. This necessitates determining if the SC's SOC is below the prescribed upper limit. The excess energy is subsequently charged to the SC if this requirement is satisfied. As seen in Fig. (14), the SC's SOC rises from 0% to 7% during this process, demonstrating that the SC is successfully storing the extra energy generated by the wind power. Since the grid is not needed to provide or receive any power throughout this charging process, it stays dormant. The grid power stays at zero as a result. To ensure that no more renewable energy is wasted, the H-STATCOM energy management system gives priority to charging the SC when the battery reaches its maximum state of charge. This mode of operation preserves system stability and efficiency while optimizing the use of available renewable energy. In addition to preventing the reduction of renewable energy, the system also prepares the SC for future discharge when quick power supply is needed by strategically charging the SC with excess energy. This mode increases the system's self-sufficiency and lessens dependency on external power sources by keeping the grid idle.

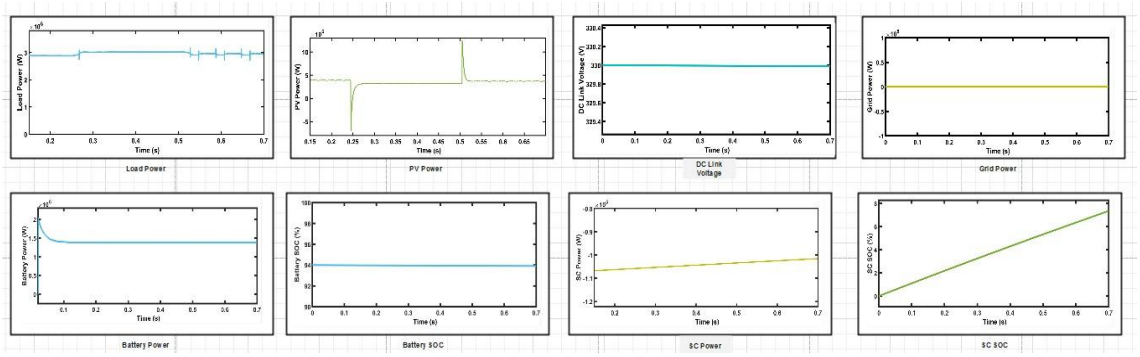

Fig.14 H-STATCOM Operation – Mode 5

Operation of Mode 6 : When the load power is less than the solar power, as shown in Fig. (15), there is extra energy available in the system. In this situation, 1 MW of surplus electricity is available, as shown in Table 8. Typically, additional energy is used to charge the battery and supercapacitor (SC), as long as their state of charge (SOC) levels are less than their respective maximums. However, if both the battery and the SC are fully charged and unable to absorb any extra energy, the excess energy is sent to the grid. In this operational mode, once the battery and SC reach their full SOC limits, the grid is the principal beneficiary of the extra energy, ensuring that no available renewable energy is wasted. The grid absorbs excess electricity to balance the system, functioning as a buffer when other energy storage components are fully charged. In this mode, the H-STATCOM does not work actively, and so the DC link voltage within the device is 0. This means that the energy storage components do not participate in the power exchange, and the grid is completely responsible for managing excess energy. This operating method allows the system to make the best use of renewable energy while ensuring system stability, even when local storage resources are completely charged. By diverting extra energy to the grid, the system improves its efficiency and ensures that renewable energy is continuously integrated into the broader power grid.

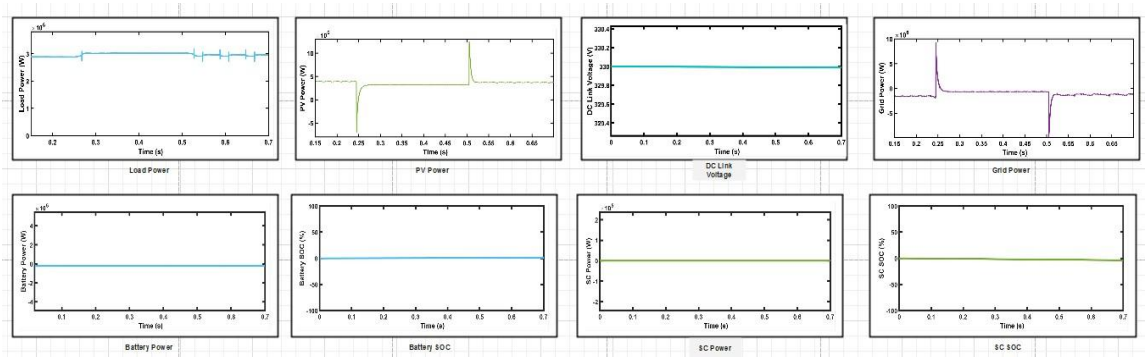

Fig. 15 H-STATCOM Operation – Mode 6

III. Results and Discussions

An analysis of power flow looks into the effects of increasing PV system use. Since the PV is likewise taken into consideration at node 18, the H-STATCOM is taken into consideration there as well. Therefore, the point of common coupling (PCC) is node 18. The PV's maximum capacity is 3.2 MW, and measurements were conducted under various solar irradiance circumstances.

A. Impacts on System Harmonics

A sinusoidal voltage or current signal with frequencies that are integer multiples of the signal's nominal frequency is called a harmonic [15]. Non-linear loads are the main source of harmonics in traditional distribution networks. According to Table 9, the following nodes are taken into consideration for analysis: Nodes 4, 18, 28, 29, 30, 31, 32, and 33. The PCC node is node 18. The source node is regarded as node 4. The load nodes are nodes 28 through 33. With the exception of Nodes 4, 18, and 33, the voltage THD for the Conventional System, which does not include PV, is less than 5% at every node taken into consideration. At Nodes 4, 18, and 33, the voltage THD is 4.13%, 4.32%, and 63.64%, respectively. Except for Node Node 33 (5.65%), the current THD is below the recommended level at all other nodes. The inclusion of PV at Node 18 increases the harmonics at each node. Especially at Node 33, with 112% voltage THD and 6.58% current THD. The IEEE 519 standard requires that the voltage and current THD be less than 5% for the power system to operate smoothly and reliably [15]. H-STATCOM is used to improve harmonics in the system by connecting to Node 18. Table 9 shows that the voltage and current THD are less than 5% at each node under consideration during H-STATCOM operation.

B. Impacts on System Power

Power changes in conventional electrical networks are mostly produced by the switching of large, nonlinear loads. This phenomena causes substantial changes in both active power and frequency, as measured at certain nodes throughout the system. For example, Node 18, known as the Point of Common Coupling (PCC), is an important point for studying these dynamics. These fluctuations are represented in Fig. 16, emphasizing the inherent difficulties in maintaining power quality and stability in traditional power systems. The integration of PV systems into the traditional network adds another degree of complication. While PV adds renewable energy to the system, its intermittent nature exacerbates power fluctuations.

Table 9 THD analysis for effects of PV

Node No.	Without PV		With PV		With PV and H-STATCOM	
	Voltage THD (%)	Current THD (%)	Voltage THD (%)	Current THD (%)	Voltage THD (%)	Current THD (%)
4	4.13	0.50	15.52	1.39	3.95	0.31
18	4.32	0.01	17.34	9.37	0.83	0.69
28	2.85	1.07	10.30	1.95	1.85	0.81
29	2.81	1.07	10.95	1.99	2.09	0.80
30	2.44	1.26	8.69	2.32	1.07	0.78
31	1.98	0.97	6.78	1.75	1.87	0.86
32	1.91	1.03	6.33	1.84	1.64	0.84
33	54.63	5.65	112.00	6.58	9.42	4.87

This intermittency is caused by fluctuations in PV irradiation, which have a effect on the solar PV system's power output. As a result, sudden fluctuations in power output are noticed, indicating a mismatch between generation and load. These mismatches emerge as power swings, which further destabilize the system, as depicted in Fig. 17. H-STATCOM successfully stabilizes the system by adjusting for power mismatches induced by load switching and solar intermittent operation. This is accomplished by storing excess energy during periods of surplus generation and then discharging it during periods of deficit. As a result, power and frequency variations are greatly minimized, bringing them into acceptable range for grid operation. Fig. 18 shows the system's increased stability during H-STATCOM operation, demonstrating its efficiency in controlling power variability at Node 18 (PCC).

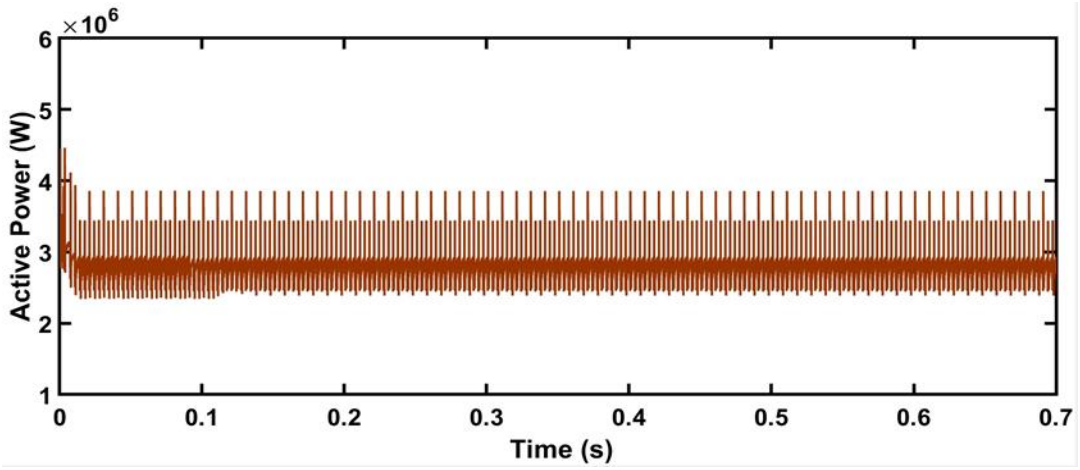

Fig. 16 Without PV Integration - Active Power at Node 18

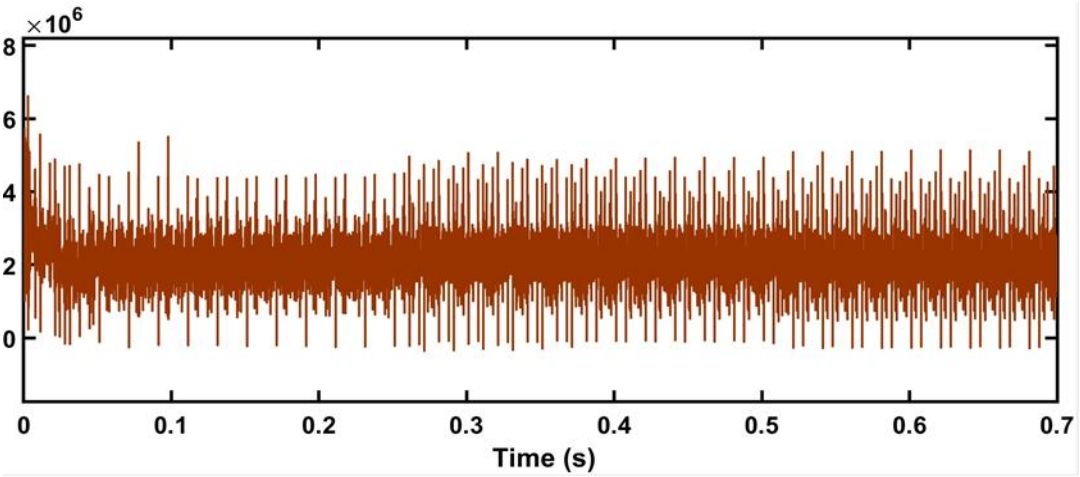

Fig. 17 With PV Integration – Active Power at Node 18

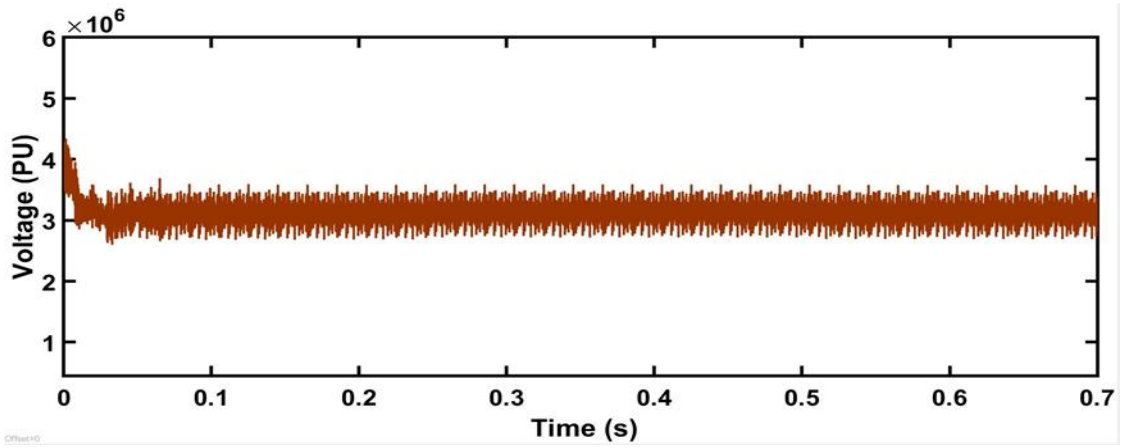

Fig. 18 With PV and H-STATCOM Integration – Active Power at Node 18

C. Effects on System Voltage

Fig. 19 shows the voltage profile (in per unit, PU) at various nodes (from node 4 to node 33) under three different operational conditions: There is no PV system, PV is present, and PV is combined with the Hybrid Energy Storage System (HESS)-based STATCOM.

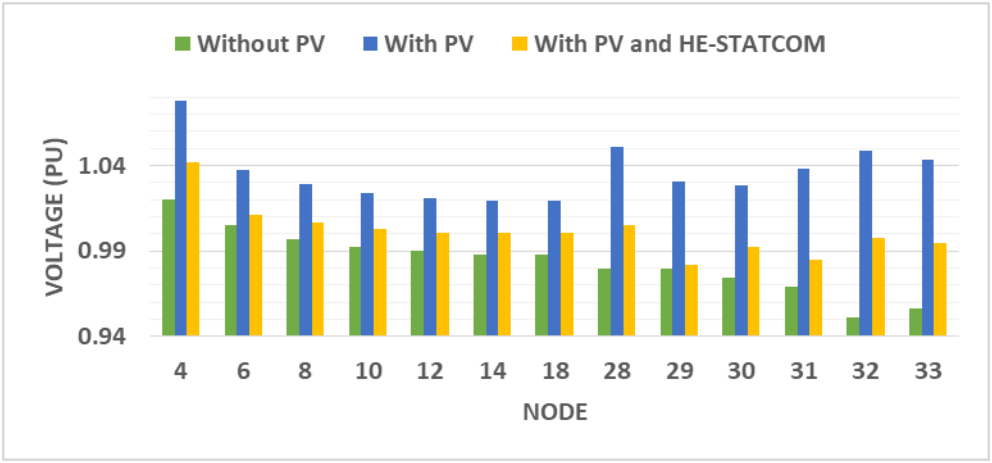

Fig. 19 Comparison of Voltage Profile under Different Scenarios

The green bar depicts the system's voltage profile in the absence of solar energy integration. The voltage is relatively low across all nodes, sitting just below 1.0 PU. The progressively increasing voltage reduction indicates that without renewable integration, the system experiences large voltage dips, which are most noticeable at nodes farthest from the source. The blue bar depicts the voltage profile once the PV is integrated. The addition of PV significantly improves voltage levels across most nodes when compared to the non-PV scenario. For nodes 4–18, the voltage remains over 1.0 PU, indicating that the solar energy contribution helps keep the voltage close to desired values. The yellow bar depicts the system's overall voltage characteristics while both PV and H-STATCOM are activated. This combination improves voltage stability in all nodes. The voltage outputs are continuously close to 1.0 PU, and node transitions are smoother than with PV alone. The addition of H-STATCOM appears to fix the voltage drop observed between nodes 18 and 28, resulting in a more consistent, reliable, and stable voltage profile, especially in the network's middle and lower regions.

The comparison of voltage performance between PV alone and PV combined with H-STATCOM across various operating scenarios—normal conditions, single line-to-ground (L-G) fault at Node 7, three-phase (L-L-L) fault at Node 15, and load switching—shows that H-STATCOM has a significant impact on improving voltage stability and system resilience, as shown in Table 10. Under typical operating conditions, PV alone produces somewhat higher voltage profiles at each node; however, adding H-STATCOM results in more uniform and stable voltage levels across all nodes, indicating a better ability to control and balance power flows. During the L-G fault at Node 7, the solar PV system alone experiences significant voltage dips at the impacted and neighboring nodes, but integration of H-STATCOM mitigates these voltage drops, demonstrating H-STATCOM's involvement in fault ride-through capabilities and system recovery. Similarly, when the more severe L-L-L fault at Node 15, PV alone causes significant voltage decreases

throughout the system, whereas H-STATCOM integration shows a higher ability to sustain voltage levels, indicating better fault tolerance.

Table 10 System Voltage Analysis under Different Contingencies

	With PV Only				With PV and H-STATCOM			
Node	Normal Condition	Load Switching	L-G fault @ Node 7	L-L-L fault @ Node 15	Normal Condition	Load Switching	L-G fault @ Node 7	L-L-L fault @ Node 15
4	1.201	1.055	1.038	1.040	1.050	1.036	1.021	1.024
6	1.070	1.080	1.065	1.067	1.044	1.047	1.035	1.038
8	1.066	1.074	1.058	1.060	1.039	1.046	1.029	1.032
10	1.063	1.071	1.055	1.057	1.036	1.044	1.027	1.030
12	1.061	1.070	1.053	1.055	1.028	1.043	1.026	1.029
14	1.061	1.070	1.053	1.055	1.036	1.044	1.026	1.030
18	1.064	1.071	1.054	1.056	1.040	1.048	1.029	1.032
28	1.050	1.051	1.040	1.046	1.043	1.046	1.036	1.040
30	1.046	1.043	1.030	1.038	1.021	1.029	1.011	1.020
33	1.035	1.040	1.021	1.024	1.030	1.033	1.019	1.022

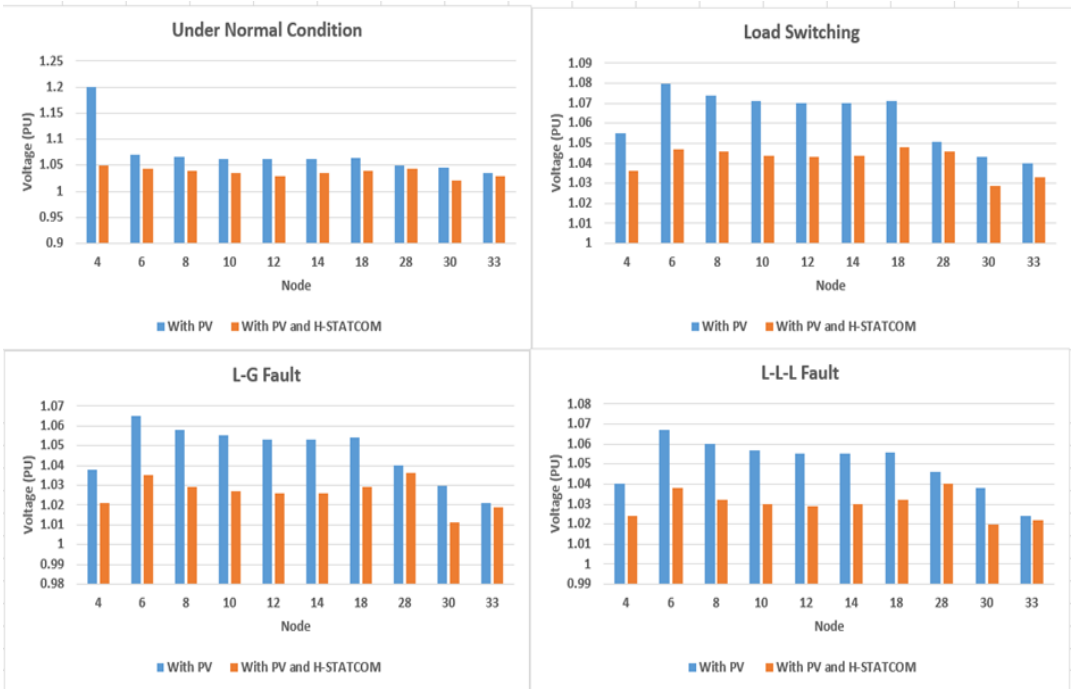

Fig. 20 Effects of PV Integration Under Contingencies

Furthermore, under load switching conditions, where the system experiences sudden changes in load demand, solar PV alone exhibits more significant voltage fluctuations, whereas the PV + H-STATCOM configuration dampens these variations, highlighting the H-STATCOM's ability to provide rapid support during transient events. Overall, incorporating H-STATCOM into a PV-based power system not only improves voltage regulation under steady-state conditions, but it also significantly increases the system's robustness during faults and dynamic operational events, making it an essential component for maintaining grid stability in renewable energy-dominated power systems. Fig. 20 depicts a visual study of voltage profiles across different nodes under four operating scenarios: normal conditions, load switching, L-G fault at Node 7, and L-L-L fault at Node 15, highlighting the tremendous benefits of including H-STATCOM into the PV system. Under normal circumstances, the solar system generates somewhat greater voltages, but the system with H-STATCOM provides more consistent voltage management. During both L-G and L-L-L faults, the PV + H-STATCOM system demonstrates superior fault tolerance by maintaining more consistent voltage levels than PV alone, which experiences more dramatic voltage decreases. H-STATCOM

integration reduces voltage variations in the load-switching scenario, proving its ability to improve system responsiveness to dynamic events. Overall, the use of H-STATCOM improves voltage stability and system robustness.

Voltage fluctuations are primarily induced by oscillatory and nonlinear loads, which result in conventional deviations in signal magnitude rather than unpredictable variations in the voltage envelope. These variations can compromise system stability and power quality, hence voltage regulation is a critical component of power system performance. Fig. 21, Fig. 22, and Fig. 23 compare voltage variations under three scenarios: (i) no PV System integration, (ii) with PV integrated at Node 18, and (iii) with both PV and an H-STATCOM at Node 18 respectively. Node 18 is known as a Point of Common Coupling (PCC), which is the critical point at which PV links to the grid.

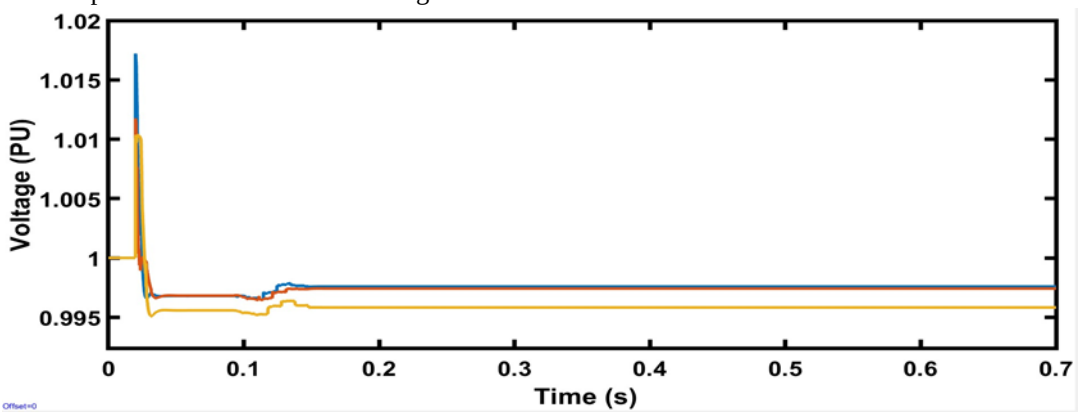

Fig. 21 Effect on Voltage Fluctuations Without PV Integration

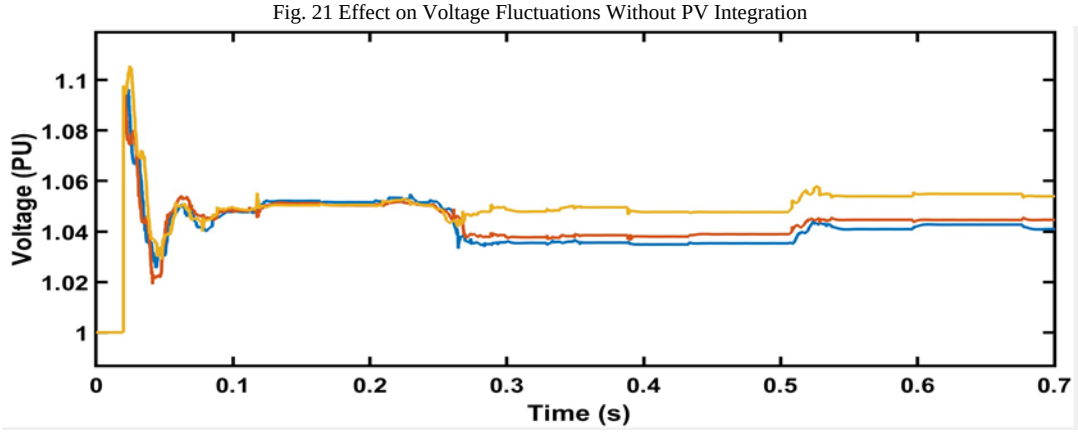

Fig. 22 Effect on Voltage Fluctuations With PV Integration

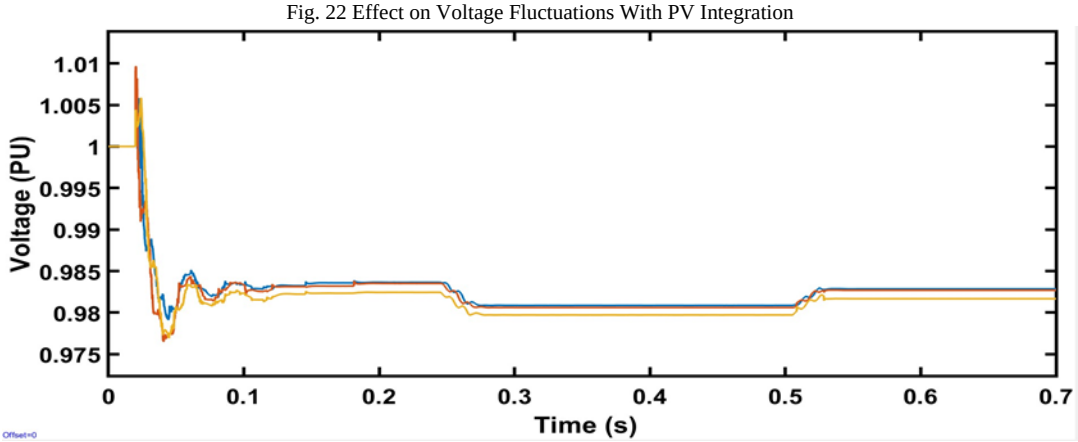

Fig. 23 Effect on Voltage Fluctuations With PV and H-STATCOM

Without the incorporation of a photovoltaic (PV) system, the voltage profile at Node 18 is stable, with values ranging from 0.95 to 0.97 PU and no noticeable variations. This stability reflects the predictable nature of conventional power systems, which keep the voltage within a specific range. However, the inclusion of a PV system has a considerable impact on voltage dynamics. Because of the intermittent and fluctuating nature of solar irradiation, the voltage profile begins to show significant swings. Simulations at different insolation levels (1000 W/m², 200 W/m², and 600 W/m²) show fluctuation, with a peak voltage of around 1.1 PU. Such elevated voltage levels, if not controlled, can undermine the stability of the electricity

system, especially in a weak grid. A hybrid static synchronous compensator (H-STATCOM), which stabilizes the voltage profile and provides dynamic reactive power compensation, is integrated into the system to address these issues. By limiting the maximum voltage to 0.985 PU and reducing voltage fluctuations, the H-STATCOM greatly improves the situation as compared to PV-only. The efficiency of H-STATCOM in preserving system stability in the presence of extensive renewable energy sources is demonstrated by this regulation, which makes sure the voltage stays within allowable bounds.

IV. Conclusion

This article provides a thorough assessment of the power quality issues that result from integrating solar PV systems into conventional electrical distribution networks. The key concern is the negative effects of harmonics, voltage profiles, voltage shifts, power fluctuations, and frequency instability caused by large-scale renewable energy integration. MATLAB Simulink is used to model and simulate the behavior of wind energy systems under different solar irradiance level scenarios. The Modified IEEE 33-node radial distribution test system is used to simulate a typical power distribution network for comparison purposes. The study aims to determine how PV system integration affects node-level power quality, including voltage stability and harmonic distortions. One of the main conclusions of the study is that after PV integration, there were noticeable voltage spikes on every node in the distribution network. The primary cause of these voltage spikes is the PV system's intrinsic erratic and dynamic insolation levels. In addition to increasing volatility in power supply, the intermittent nature of PV necessitates the use of power electronic converters to transform wind turbines' unexpected output into grid-compatible electricity. Nonetheless, these converters contribute to the power system's harmonic introduction and increased voltage fluctuations, which can degrade system performance and overall power quality. However, these converters are responsible for the power system's harmonic introduction and magnified voltage swings, which can degrade system performance and overall power quality. The study proposes integrating H-STATCOM into the distribution network to address power quality issues that develop as a result of PV integration. The H-STATCOM consists of two components: supercapacitors (SCs) and battery storage, which operate together to provide complementary advantages in terms of quick power response and energy storage. The supercapacitor is skilled at dealing with power imbalances, but battery storage can store energy for extended periods of time and smooth out power supply oscillations. The power quality disturbances caused by PV integration are significantly mitigated by this hybrid system, particularly when it comes to suppressing harmonics and reducing voltage and power fluctuations. A traditional power management algorithm is also included in the research to increase the operating efficiency and dependability of the energy storage system. This algorithm, which dynamically manages each component's charge and discharge cycles based on current power system conditions, is critical for the battery-supercapacitor H-STATCOM's optimal operation. The algorithm extends the life of the energy storage components by restricting overcharging and deep draining of the devices, hence reducing undue stress on them while in use. This approach also optimizes the flow of energy throughout the system, ensuring that energy conserved is efficiently dispatched when needed and that energy storage capacity is available for unforeseen future events. This study lacks the incorporation of artificial strategies for smoothing out the power management process.

Nomenclature

I_{op} = output current of PV system (A)
N_{cp} = no. of PV cells in series
I_{sc} = short circuit current of PV module (A)
k_i = temperature coefficient of I_{sc} (A/˚C)
T = PV array temperature (˚C)
G = Solar Insolation (W/m^2)
N_{cp} = no. of PV cells in parallel
I_o = diode saturation current (A)
v = PV system output voltage (V)
R_{se} = series resistance of PV module (Ω)
R_{pa}= shunt resistance of PV module (Ω)
q = electron charge (C)
V_t = thermal voltage (V)
I_{rs} = diode reverse saturation current (A)
N_T = no. of total PV modules required
V_{M_PV} = maximum voltage PV array (V)
I_{M_PV}= maximum current of PV array (A)
V_{OC_PV} = open circuit voltage of PV array (V)
I_{SC_PV} = short circuit current of PV array (A)
N_{SC_S} = no. of SC cells in series
N_{SC_P} = no. of SC cells in parallel
V_{SC} = Voltage of SC array (V)
V_B = Voltage of Battery array (V)
C_{SC_t} = total capacitance of SC array (F)
E_{SC_t}= total energy required for SC array (J)
N_{B_S}= no. of battery cells in series
N_{B_P}= no. of battery cells in parallel
E_{B_t} = total energy required for battery array (J)

k = Boltzmann's constant
A = Ideality factor
N_{pp} = no. of PV modules in parallel
N_{ps}= no. of PV modules in series
I_{Bat} = Battery array current (A)
I^{*}_{Bat}= Reference current for Battery array (A)
I^{*}_{SC} = Reference current for SC array (A)
I_{SC} = SC array current (A)

CONFLICT OF INTEREST

THE AUTHOR (S) DECLARE (S) THAT THERE IS NO FINANCIAL AND NON-FINANCIAL CONFLICT OF INTEREST.

FUNDING STATEMENT

THE AUTHOR (S) DECLARE (S) THAT THIS RESEARCH DOES NOT RECEIVE ANY FUNDING.

DATA ACCESS STATEMENT

THE AUTHOR (S) DECLARE (S) THAT NO NEW DATA HAS BEEN PRODUCED FOR THIS RESEARCH.

ETHICS STATEMENT

THE AUTHOR (S) DECLARE (S) THERE IS NO ETHICAL APPROVAL IS APPLICABLE.

REFERENCES

[1] Shafiullah, M., Ahmed, S. D., & Al-Sulaiman, F. A. . Grid integration challenges and solution strategies for solar PV systems: a review. IEEE Access, 10, 52233-52257 (2022)
[2] Central Electricity Authority, Government of India, 2024 Dashboard - Central Electricity Authority (CEA.nic.in) (2024). Accessed on 3 June,2024
[3] Tür, M. R., Mohammed, W., SHOBOLE, A. A., & Gündüz, H. Integration problems of photovoltaic systems-wind power, solutions and effects on power quality. European Journal of Technique (EJT), 10(2), 340-353 (2021)
[4] Alkahtani AA, Alfalahi ST, Athamneh AA, Al-Shetwi AQ, Mansor MB, Hannan MA, Agelidis VG. Power quality in microgrids including supra harmonics: Issues, standards, and mitigations. IEEE Access, 8:127104-22 (2020)
[5] Bajaj M, Singh AK. Grid integrated renewable DG systems: A review of power quality challenges and state-of-the-art mitigation techniques. International Journal of Energy Research, 44(1):26-69 (2020)
[6] Jha K, Shaik AG. A comprehensive review of power quality mitigation in the scenario of solar PV integration into the utility grid. e-Prime-Advances in Electrical Engineering, Electronics and Energy, 100103 (2023)
[7] Satyanarayana, P. V. V., Radhika, A., Reddy, C. R., Pangedaiah, B., Martirano, L., Massaccesi, A., ... & Jasiński, M. Combined DC-link fed parallel-VSI-based DSTATCOM for power quality improvement of a solar DG integrated system. Electronics, 12(3), 505 (2023)
[8] Awaar, V. K., Jugge, P., Kalyani, S. T., & Eskandari, M. Dynamic voltage restorer–a custom power device for power quality improvement in electrical distribution systems. In Power Quality: Infrastructures and Control, Singapore, pp 97-116 (2023)
[9] Dutta, A. K., Bharathi Krishna, L., Rayudu, K., Vedhagiri, D., Medikondu, N. R., SudarsananNair JalajaKumari, S. P., ... & Saha, N. Battery-Based Energy Storage and Solar Technologies Integrated for Power Matching and Quality Improvement Using Artificial Intelligence. Electric Power Components and Systems, 52(2), 322-336. (2024)
[10] Villa-Ávila, E., Arévalo, P., Aguado, R., Ochoa-Correa, D., Iñiguez-Morán, V., Jurado, F., & Tostado-Véliz, M. Enhancing Energy Power Quality in Low-Voltage Networks Integrating Renewable Energy Generation: A Case Study in a Microgrid Laboratory. Energies, 16(14), 5386 (2023)
[11] Bhavya, K., Sujatha, B., & Subhashitha, P. Power Quality Enhancement in Distribution System Using Ultracapacitor Integrated Power Conditioner. In Proceedings of Fourth International Conference on Computer and Communication Technologies: IC3T, Singapore, pp. 601-612 (2022)
[12] Arifin, E. A., Sulaeman, I., Moonen, N., & Popović, J. Hybrid Energy Storage System in Microgrid to Improve Power Quality in Indonesia's Remote Area. In 2023 IEEE 7th Global Electromagnetic Compatibility Conference (GEMCCON), pp. 21-22 (2023)
[13] Chen, S., Yu, B., Weng, L., Zhou, G., & Han, R. Hybrid Storage System Planning for Power Quality Improvement in Power Distribution System with Solar Photovoltaic Sources. In International Conference on Frontier Computing, Singapore: Springer Nature Singapore, pp. 655-661 (2021)
[14] Lenka, S., Sinha, P., & Jena, C. A review on power quality improvement of grid connected PV with lithium-ion and super capacitor based hybrid energy storage system using a new control strategy. Renewable Energy Optimization, Planning and Control: Proceedings of ICRTE, Volume 1, 1-10 (2022)
[15] Abdalla, A. A., El Moursi, M. S., El-Fouly, T. H., & Al Hosani, K. H. A novel adaptive power smoothing approach for PV power plant with hybrid energy storage system. IEEE Transactions on Sustainable Energy, 14(3), 1457-1473 (2023)